Toxicology and Applied Pharmacology 485 (2024) 116911

Contents lists available at ScienceDirect

Toxicology and Applied Pharmacology

journal homepage: www.elsevier.com/locate/taap

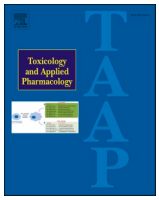

The ABCB1 and ABCG2 efflux transporters limit brain disposition of the SYK inhibitors entospletinib and lanraplenib

Nancy H.C. Loos [a], Rolf W. Sparidans [b], Paniz Heydari [b], Viët Bui [a], Maria C. Lebre [a], Jos H. Beijnen [a,c,d], Alfred H. Schinkel [a,*]

[a] The Netherlands Cancer Institute, Division of Pharmacology, Amsterdam, the Netherlands
[b] Utrecht University, Faculty of Science, Department of Pharmaceutical Sciences, Division of Pharmacology, Utrecht, the Netherlands
[c] Utrecht University, Faculty of Science, Department of Pharmaceutical Sciences, Division of Pharmacoepidemiology and Clinical Pharmacology, Utrecht, the Netherlands
[d] The Netherlands Cancer Institute, Division of Pharmacy and Pharmacology, Amsterdam, the Netherlands

ARTICLE INFO

Editor: Lawrence Lash

Keywords:
Entospletinib
Lanraplenib
SYK inhibitor
ABCB1/P-glycoprotein
ABCG2/Breast cancer resistance protein

ABSTRACT

The highly selective Spleen Tyrosine Kinase (SYK) inhibitors entospletinib and lanraplenib disrupt kinase activity and inhibit immune cell functions. They are developed for treatment of B-cell malignancies and autoimmunity diseases. The impact of P-gp/ABCB1 and BCRP/ABCG2 efflux transporters, OATP1a/1b uptake transporters and CYP3A drug-metabolizing enzymes on the oral pharmacokinetics of these drugs was assessed using mouse models. Entospletinib and lanraplenib were orally administered simultaneously at moderate dosages (10 mg/kg each) to female mice to assess the possibility of examining two structurally and mechanistically similar drugs at the same time, while reducing the number of experimental animals and sample-processing workload. The plasma pharmacokinetics of both drugs were not substantially restricted by Abcb1 or Abcg2. The brain-to-plasma ratios of entospletinib in *Abcb1a/b*$^{-/-}$, *Abcg2*$^{-/-}$ and *Abcb1a/b;Abcg2*$^{-/-}$ mice were 1.7-, 1.8- and 2.9-fold higher, respectively, compared to those in wild-type mice. For lanraplenib these brain-to-plasma ratios were 3.0-, 1.3- and 10.4-fold higher, respectively. This transporter-mediated restriction of brain penetration for both drugs could be almost fully inhibited by coadministration of the dual ABCB1/ABCG2 inhibitor elacridar, without signs of acute toxicity. Oatp1a/b and human CYP3A4 did not seem to affect the pharmacokinetics of entospletinib and lanraplenib, but mouse Cyp3a may limit lanraplenib plasma exposure. Unexpectedly, entospletinib and lanraplenib increased each other's plasma exposure by 2.6- to 2.9-fold, indicating a significant drug-drug interaction. This interaction was, however, unlikely to be mediated through any of the studied transporters or CYP3A. The obtained insights may perhaps help to further improve the safety and efficacy of entospletinib and lanraplenib.

1. Introduction

Spleen Tyrosine Kinase (SYK) is a cytoplasmic non-receptor kinase containing two SRC homology 2 (SH2)-domains and a kinase domain (Tang et al., 2022; Mócsai et al., 2010). SYK is expressed in various cell types, including hematopoietic cells (such as B cells, immature T cells and macrophages) and non-hematopoietic cells (such as epithelial cells, hepatocytes and fibroblasts) (Tang et al., 2022). SYK kinase functions in multiple downstream signaling pathways facilitating various biological functions (Colucci et al., 2000; Mócsai et al., 2006; Liao et al., 2013). Signaling in which it is involved occurs through multiple immunoreceptor tyrosine-based activation motif (ITAM)-containing immunoreceptors across different immune cell types, including the B cell receptor (BCR) (Currie et al., 2014; Blomgren et al., 2020). Via its role in BCR signaling, SYK can affect the development, activation, and maturation of B cells, as well as antibody production and class switching (Blomgren

Abbreviations: ABC, ATP-binding cassette; ANOVA, analysis of variance; AUC, area under the plasma concentration-time curve; AML, acute myeloid leukemia; BBB, blood-brain barrier; BCR, B cell receptor; BCRP/ABCG2, Breast Cancer Resistance Protein; BSA, bovine serum albumin; CLL, chronic lymphocytic leukemia; C_{max}, peak plasma concentration; CYP, cytochrome P450; FVB, Friend Virus B; GVHD, graft-versus-host-disease; ITAM, immunoreceptor tyrosine-based activation motif; LC-MS/MS, liquid chromatography-tandem mass spectrometry; LN, lupus nephritis; MCL, mantle cell lymphoma; OATP/SLCO, organic anion-transporting polypeptides; P-gp/ABCB1/MDR1, P-glycoprotein; PPI, proton pump inhibitor; SD, standard deviation; SH2, SRC homology 2; SIC, small intestinal content; SLE, systemic lupus erythematosus; SYK, spleen tyrosine kinase; T_{max}, time to reach peak plasma concentration..

* Corresponding author at: Division of Pharmacology, The Netherlands Cancer Institute, Plesmanlaan 121, 1066 CX Amsterdam, the Netherlands.
E-mail address: a.schinkel@nki.nl (A.H. Schinkel).

https://doi.org/10.1016/j.taap.2024.116911
Received 23 December 2023; Received in revised form 11 March 2024; Accepted 20 March 2024
Available online 26 March 2024

et al., 2020).

Inhibition or deletion of SYK has significant inhibitory effects on the functioning of immune cells and immunity. One oral ATP-competitive SYK inhibitor that entered clinical trials is entospletinib (Suppl. Fig. 1A), which is highly selective and disrupts kinase activity with an IC_{50} of 7.6 nM (Currie et al., 2014; Ramanathan et al., 2017). Entospletinib could be beneficial for the treatment of a variety of B cell malignancies, including acute myeloid leukemia (AML), chronic lymphocytic leukemia (CLL), and mantle cell lymphoma (MCL) (Ramanathan et al., 2017; Andorsky et al., 2019). Entospletinib also showed efficacy in treating graft-versus-host-disease (GVHD) (Poe et al., 2018; Sharman et al., 2015). The clinically used oral dose is 800 mg twice daily with a median plasma half-life of 9–15 h (Currie et al., 2014; Ramanathan et al., 2017). In vivo, it showed moderate to high bioavailability in rat and dog (1 mg/kg). In vitro, entospletinib showed inhibition of BCR-mediated activation and proliferation of B-cells as well as immune-complex stimulated cytokine production in monocytes, indicating its activity in both the initiation and effector phases of inflammatory diseases (Currie et al., 2014). However, the development of entospletinib in various inflammatory disease regimens was obstructed by a drug-drug interaction with proton pump inhibitors (PPIs) due to its pH-dependent solubility (Ramanathan et al., 2017).

Another second-generation selective oral SYK inhibitor is lanraplenib (Suppl. Fig. 1B), with an IC_{50} of 120 nM (Blomgren et al., 2020). Its pharmacokinetic properties are more advantageous compared to those of entospletinib, allowing once daily administration without PPI interactions. Lanraplenib has a better solubility, independent of pH, increasing its absorption after oral administration, and it has a longer half-life (21.3–24.6 h) compared to entospletinib (Blomgren et al., 2020). In a phase II clinical study, lanraplenib was orally dosed at 30 mg once daily (Baker et al., 2020). Lanraplenib could be used for treatment of systemic lupus erythematosus (SLE) and lupus nephritis (LN) (Blomgren et al., 2020). In vitro studies showed that lanraplenib is a potent inhibitor of signaling downstream of BCR and completely abrogates the expression of cell-surface activation markers CD86 and CD69, with EC_{50} values of 112 and 164 nM. Lanraplenib also caused reduced immune-complex stimulated release of proinflammatory cytokines such as TNFα and IL-1 from human macrophages (Blomgren et al., 2020). In a study with NZB/W F1 mice, a spontaneous lupus model, lanraplenib (0.25% in chow) prevented the increase in proteinuria associated with disease progression and it improved survival of the animals (Pohlmeyer et al., 2021).

Insights into certain determinants of the pharmacokinetics of entospletinib and lanraplenib can provide important information for clinicians on drug-drug interaction profiles and drug efficacy and safety (Giacomini et al., 2010; Oesch, 2009). P-glycoprotein (P-gp/MDR1/ABCB1) and Breast Cancer Resistance Protein (BCRP/ABCG2) are important multidrug efflux transporters with broad substrate specificities (Schinkel and Jonker, 2003). Mouse Abcb1a and Abcb1b (two paralogous genes) have 83% sequence similarity with human ABCB1 (single gene) and they have extensive overlapping functions with the human ortholog (Devault and Gros, 1990). This identity is 86% between murine Abcg2 (single gene) and ABCG2 (single gene) (Allen et al., 1999). These ABC transporters reside primarily in the luminal (apical) membrane of polarized cells of multiple organs, especially in the liver, small intestine and kidneys, where they can limit intestinal absorption and facilitate direct hepatic, intestinal or renal excretion of their substrates (Giacomini et al., 2010; Choudhuri and Klaassen, 2006; Szakács et al., 2008). These ABC transporters further play an important role in restricting the brain distribution of substrate drugs due to their expression at the luminal side of the blood-brain-barrier (BBB) (Miller, 2014; Bao et al., 2020; Schinkel et al., 1996; Goncalves et al., 2018). Reduced brain exposure may impair the efficacy of their substrate drugs against brain (micro-) metastases (Schinkel et al., 1996; Goncalves et al., 2018).

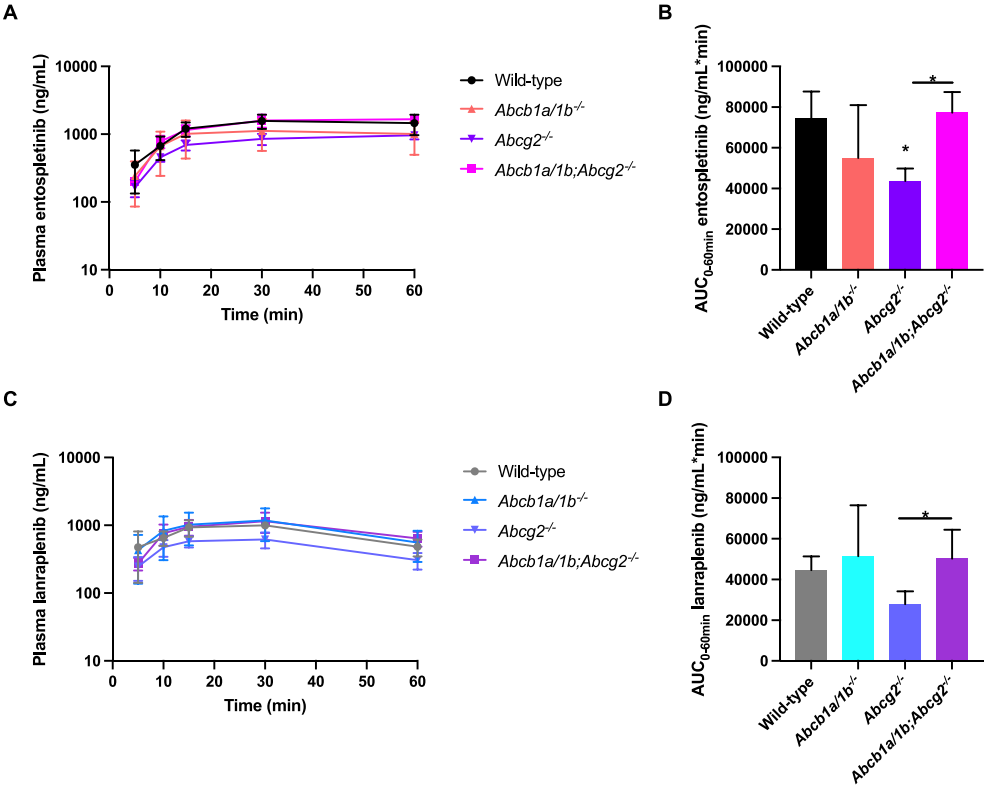

Fig. 1. Pharmacokinetic parameters in female wild-type, *Abcb1a/b*$^{-/-}$, *Abcg2*$^{-/-}$ and *Abcb1a/b;Abcg2*$^{-/-}$ mice 1 h after oral administration of 10 mg/kg entospletinib and 10 mg/kg lanraplenib simultaneously (n = 6/group). **A.** Plasma concentration-time curve of entospletinib (semi-log scale). **B.** $AUC_{0-60\ min}$ of entospletinib, area under the plasma concentration-time curve from 0 to the last time point (t = 60 min). **C.** Plasma concentration-time curve of lanraplenib (semi-log scale). **D.** $AUC_{0-60\ min}$ of lanraplenib. Data are presented as mean ± SD. *, $P < 0.05$ compared to wild-type mice or as indicated by the bar.

SYK inhibitor pharmacokinetics might further be affected by uptake transporters, such as the organic anion-transporting polypeptides (OATPs; SLCO) which mediate the cellular influx of many drugs. Especially the liver uptake of substrate drugs can be facilitated by the subfamily members OATP1B1 and OATP1B3, which are primarily expressed in the sinusoidal membrane of hepatocytes (Kalliokoski and Niemi, 2009; Couto et al., 2020).

Also drug-metabolizing enzymes can influence the oral availability of their substrate drugs. CYP3A4, an important member of the Cytochrome P450 (CYP) superfamily, is expressed in the human liver and small intestine (Lolodi et al., 2017; Zanger and Schwab, 2013). CYP3A4 has a broad substrate specificity and therefore limits the systemic exposure of a wide range of drugs (Zanger and Schwab, 2013). Moreover, this enzyme is susceptible to inhibition or induction by various drugs, as well as genetic polymorphisms, resulting in substantial inter- and intra-individual variation in enzyme activity (Lolodi et al., 2017; Zanger and Schwab, 2013; Lamba et al., 2002).

According to in vitro experiments, entospletinib is a substrate of ABCG2/BCRP and could possibly inhibit this transporter as well (Narayanan et al., 2021). A non-peer reviewed abstract on entospletinib drug-drug interactions in human volunteers further suggested that entospletinib may be metabolized by CYP3A, but not extensively under normal conditions; that it may act as an inhibitor of ABCG2 and/or OATP1B1/3; and that it may modestly inhibit ABCB1 (Dolton et al., 2016). In contrast, for lanraplenib this kind of information is still lacking.

In the current study, we hypothesized that ABC and OATP transporters, as well as the CYP3A enzyme might influence the net oral absorption and tissue distribution of entospletinib and lanraplenib, and hence their effective availability. Such information could support further optimal development of these drugs. We used Abcb1, Abcg2, Oatp1a/b, and Cyp3a knockout and CYP3A4 transgenic mouse strains to investigate this impact. Furthermore, we also wanted to determine if it is possible to use fewer experimental mice by simultaneously examining two drugs with related structures and mechanism of action at the same time in our mouse models. When this latter principle turns out to be feasible, it could be applied more often, in order to reduce the number of mice needed in experiments and thus increase breeding flexibility, and reduce the amount of experimental work involved in sample processing.

2. Materials and methods

2.1. Chemicals

Entospletinib was purchased from MedKoo Biosciences (Morrisville, NC) and lanraplenib from MedChem Express (Monmouth Junction, NJ). Elacridar HCl was obtained from Biosynth (Bratislava, Slovakia). Bovine Serum Albumin (BSA) Fraction V was supplied by Roche Diagnostics (Mannheim, Germany). Isoflurane was purchased from Virbac Nederland (Barneveld, The Netherlands) and heparin (5000 IU·mL^{-1}) from Leo Pharma (Breda, The Netherlands). All other reagents and chemicals used were supplied by Sigma-Aldrich (Steinheim, Germany).

2.2. Animals

Housing and handling of the mice were according to institutional guidelines complying with Dutch and EU legislation. All experimental animal protocols (under national permit number AVD30100202114776) used for this study, were approved on July 2021 and October 2022 by the institutional board for care and use of laboratory animals. Female wild-type, *Abcb1a/1b*$^{-/-}$, *Abcg2*$^{-/-}$, *Abcb1a/1b; Abcg2*$^{-/-}$, *Oatp1a/b*$^{-/-}$, *Cyp3a*$^{-/-}$, and Cyp3aXAV (*Cyp3a*$^{-/-}$ mice with overexpression of human CYP3A4 in liver and intestine) mice were used for the pharmacokinetics studies. Female mice were used in these experiments, because autoimmunity syndromes are more prevalent in women. Moreover, by Dutch/EU law mice generated by breeding need to be used optimally, and parallel generated male mice were used for studies on a prostate cancer drug. Every group consisted of 6 mice and all animals were of a > 99% FVB genetic background. Their age varied between 9 and 13 weeks. Mice received a standard diet (Transbreed, SDS Diets, Technilab-BMI, Someren, The Netherlands) and acidified water ad libitum. Mice were kept in a specific pathogen-free, temperature-controlled environment with a 12-h light and 12-h dark cycle. Animal welfare assessments were performed before, during, and after the experiments.

2.3. Oral drug solutions

Entospletinib and lanraplenib were dissolved in DMSO at a concentration of 10 mg/mL. This stock solution was further diluted 10-fold with cremophor EL and water to yield a final concentration of entospletinib and lanraplenib each of 1 mg/mL in the drug solution for oral administration [DMSO, cremophor EL, and water ratios 1:1:8 (*v*/v/v)]. This formulation was used for the single administration of either drug and for a combined administration of these drugs at the same time. For the pharmacokinetic boosting study, elacridar HCl was dissolved in DMSO at 53 mg/mL to obtain 50 mg elacridar base per mL. The elacridar stock solution was 10-fold diluted with a mixture of polysorbate 80, ethanol and water [20:13:67 (*v*/v/v)], to yield an elacridar concentration of 5 mg/mL in the oral dosing solution. The dosing solutions were freshly made on the day of the experiments.

2.4. Pharmacokinetic study of entospletinib and lanraplenib in mice

Before the start of the experiment, mice were fasted for 2–3 h to minimize variation in oral drug absorption. Entospletinib (10 mg/kg of body weight; 1 mg/mL dosing solution) and lanraplenib (10 mg/kg of body weight; 1 mg/mL dosing solution) were orally administered by gavage into the stomach using a blunt-ended needle. In this 60 min experiment, female wild-type, *Abcb1a/1b*$^{-/-}$, *Abcg2*$^{-/-}$ and *Abcb1a/1b; Abcg2*$^{-/-}$ mice were used. A second 60 min experiment was performed in female wild-type and *Oatp1a/b*$^{-/-}$ mice. Blood samples (~50 μL per sample) were taken from the tail vein using heparinized microvettes at 5, 10, 15, and 30 min after entospletinib and/or lanraplenib administration. In a 4 h experiment, female wild-type *Cyp3a*$^{-/-}$ and Cyp3aXAV mice were used. Blood samples in this experiment were collected at 7.5, 15, and 30 min, and 1 and 2 h after administration of the drugs. At the final time points of 60 min or 4 h, mice were anesthetized using an evaporator with isoflurane (3%), 0.8 L/min air and 0.3 L/min oxygen. The final blood samples were collected by cardiac puncture using a heparinized needle and syringe. Subsequently, the experiment was terminated by cervical dislocation of the anesthetized mice. The brain, liver and small intestinal content (SIC) were collected. The SIC was collected by separation from the small intestinal tissue. Blood samples were centrifuged at 9000 x*g* for 6 min at 4 °C to separate the plasma from the blood. All plasma fractions were stored at −30 °C until analysis. Brain, liver and SIC were homogenized in a FastPrep-24TM 5G homogenizer (M.P. Biomedicals, Santa Ana, CA) for 1 min using 1, 3 and 2 mL of 2% (*w*/*v*) BSA, respectively. All tissue samples were stored at −80 °C until analysis.

2.5. Pharmacokinetic boosting study with orally administered elacridar

Oral administration of elacridar (50 mg/kg of body weight; 5 mg/mL dosing solution) to wild-type mice was three hours prior to entospletinib and lanraplenib administration. Subsequently, all mice were fasted for at least 3 h. After this fasting period, oral administration of entospletinib (10 mg/kg of body weight; 1 mg/mL dosing solution) and lanraplenib (10 mg/kg of body weight; 1 mg/mL dosing solution) was performed as described above. Blood sampling and tissue collection was performed as described above. Processing and storage of the samples were as described above as well.

2.6. Bioanalytical analysis

A recently developed specific liquid chromatography-tandem mass spectrometry (LC-MS/MS) method was used to measure the concentrations of entospletinib and lanraplenib in plasma samples and tissue homogenates. Proteins were precipitated from 10 μL of sample by adding 20 μL acetonitrile (containing 10 mg/mL erlotinib as internal standard) and vortex mixing. Next, proteins were separated by centrifugation for 5 min at 2643 x*g* and ambient temperature. Of the resulting supernatant, 20 μL was further diluted with 200 μL 25% (*v*/v) methanol before analysis.

Samples were injected (0.5 μL for brain samples, 1 μL for other matrices) onto a Waters Acquity UPLC® BEH C18 column (30 × 2.1 mm, d_p = 1.7 μm) with the corresponding precolumn for chromatographic separation applying gradient elution. The mobile phases consisted of 0.1% (v/v) ammonium hydroxide in water (A) and methanol (B). Detection was carried out on a AB SCIEX QTRAP® 5500 triple quadrupole mass spectrometer with electrospray ionization operating in the positive ion mode. Calibration curves of entospletinib and lanraplenib were used in the range of 2–2000 ng/mL.

2.7. Pharmacokinetic calculations and statistical analysis

Non-compartmental analysis was used to calculate the pharmacokinetic parameters using the software package of PK solutions 2.0.2 (SUMMIT, Research Service, Montrose, CO). The area under the curve (AUC) was calculated using the linear trapezoidal rule without extrapolating to infinity. The raw data of each individual mouse were used to extract the peak plasma concentration (C_{max}) and time of peak plasma concentration (T_{max}). Tissue-to-plasma ratios were first calculated for each individual mouse, and then the mean and SD of these individual tissue-to-plasma ratios per experimental group was presented. The recovery of drug from the small intestinal contents was expressed as the percentage of the dose given to each individual mouse, since mice received slightly different absolute amounts of drug depending on their body weights. Graphs were drawn with GraphPad Prism 9 (GraphPad Software, La Jolla, CA), including the performance of the statistical analysis. The two-sided unpaired Student *t*-test was performed for the comparison of two groups. When multiple groups were compared, one-way analysis of variance (ANOVA) was applied, whereas Sidak's post hoc correction was used to account for the multiple comparisons. In view of the often large differences in means and standard deviations between groups, data were first log-transformed before applying statistical analysis. Differences were considered statistically significant, when $P < 0.05$. All data are presented as geometric mean ± SD.

3. Results

3.1. Plasma pharmacokinetics of entospletinib and lanraplenib

The impact of ABC transporters was assessed in a 60 min oral administration experiment using wild-type, *Abcb1a/1b*$^{-/-}$, *Abcg2*$^{-/-}$, and *Abcb1a/1b;Abcg2*$^{-/-}$ mice. A relatively short termination time was chosen to ensure relatively high tissue levels of the drugs at the time of termination. All four strains received the two drugs (10 mg/kg each) simultaneously in one formulation, except for wild-type mice which also received either entospletinib or lanraplenib alone (at 10 mg/kg).

In the combined administration arm, there were no significant differences in entospletinib plasma $AUC_{0–60min}$ between wild-type, *Abcb1a/1b*$^{-/-}$ and *Abcb1a/1b;Abcg2*$^{-/-}$ mice (Fig. 1A-B, Suppl. Table 1). However, the plasma $AUC_{0–60min}$ of entospletinib was 1.7-fold lower in the *Abcg2*$^{-/-}$ compared to wild-type mice, and it was also significantly lower than that in *Abcb1a/1b;Abcg2*$^{-/-}$ mice ($P < 0.05$ for each, Fig. 1A-B, Suppl. Table 1). The C_{max} of entospletinib showed a similar pattern with slightly higher significance rates (Suppl. Table 1). These results suggest that there is probably no influence of Abcb1 on the plasma exposure of entospletinib and perhaps a minimal role for Abcg2. However, experimental variation may also play a role, especially when compared to *Abcg2*$^{-/-}$ mice, since *Abcb1a/1b;Abcg2*$^{-/-}$ mice, which also lack Abcg2, were not significantly different from wild-type or *Abcb1a/1b*$^{-/-}$ mice (Fig. 1A-B). It is also mechanistically unexpected that absence of Abcg2 would decrease the plasma level of a putative substrate, rather than increase it. The overall plasma exposure of lanraplenib in the combination administration arm was slightly lower (1.7-fold in wild-type mice) compared to that of entospletinib (Fig. 1, Suppl. Table 1). The plasma $AUC_{0–60min}$ of lanraplenib was not significantly different in all three ABC transporter-deficient strains compared to wild-type mice (Fig. 1C-D, Suppl. Table 1). However, also for lanraplenib the $AUC_{0–60min}$ of *Abcg2*$^{-/-}$ mice was slightly reduced compared to *Abcb1a/1b*$^{-/-}$ and *Abcb1a/1b;Abcg2*$^{-/-}$ mice (both 1.8-fold, $P < 0.05$, Fig. 1C-D, Suppl. Table 1). Overall, the AUC profiles for entospletinib and lanraplenib across the different strains and conditions were very similar (compare Fig. 1B and D), so any experimental variation, for instance due to different stomach emptying rates, may have equally affected the plasma AUCs of entospletinib and lanraplenib in the *Abcg2*$^{-/-}$ mice.

3.2. Tissue disposition of entospletinib and lanraplenib

The influence of ABCB1 and ABCG2 on the tissue disposition of entospletinib and lanraplenib was subsequently studied. Especially in the brain, we observed a strong impact of these efflux transporters. The brain-to-plasma ratio of entospletinib in *Abcb1a/1b;Abcg2*$^{-/-}$ was 2.9-fold ($P < 0.0001$) higher than that in wild-type mice (Fig. 2A-B, Suppl. Table 1). In the single Abcb1a/1b-deficient mice this enhancement of the brain-to-plasma ratio was 1.7-fold ($P < 0.01$) and in the Abcg2-deficient mice 1.8-fold ($P < 0.001$, Fig. 2B, Suppl. Table 1). These data indicate that the brain exposure of entospletinib is significantly (and similarly) restricted by both Abcb1 and Abcg2 activity.

The impact of the ABC transporters was even more prominent in the brain exposure of lanraplenib. We observed a 10.4-fold ($P < 0.0001$) increase in brain-to-plasma ratio of lanraplenib in *Abcb1a/1b;Abcg2*$^{-/-}$ compared to wild-type mice (Fig. 2C-D, Suppl. Table 1). For lanraplenib, there was a more pronounced impact for Abcb1a/1b alone compared to Abcg2, resulting in a 3-fold ($P < 0.0001$) enhancement of the brain-to-plasma ratio in *Abcb1a/1b*$^{-/-}$ compared to wild-type mice (Fig. 2D, Suppl. Table 1). In contrast, there was no significant difference between *Abcg2*$^{-/-}$ and wild-type mice regarding the brain exposure. However, the highly significant 3.5-fold higher brain-to-plasma ratio of lanraplenib in *Abcb1a/1b;Abcg2*$^{-/-}$ compared to *Abcb1a/1b*$^{-/-}$ mice still clearly indicates a role of Abcg2 in reducing lanraplenib brain penetration when Abcb1 is absent.

Interestingly, the recovered percentage of the dose (as administered to each individual mouse) in the small intestinal content (SIC) did not seem to be much affected by the ABC transporters for either drug (Suppl. Fig. 2A and C). This suggests that the intestinal excretion of entospletinib and lanraplenib and/or their net intestinal absorption is not strongly influenced by Abcb1 or Abcg2. The recovered percentage of dose-to-AUC ratio of lanraplenib in *Abcb1a/1b;Abcg2*$^{-/-}$ mice was slightly lower (2.0-fold, $P < 0.05$) compared to that in wild-type (Suppl. Fig. 2D). This may suggest a minor role of Abcb1 and, perhaps, Abcg2 in reducing the net absorption of lanraplenib. Although the percentage of dose recovered from the SIC was on average about 3-fold higher for entospletinib than for lanraplenib (Suppl. Fig. 2A and C), in both cases most of the administered drug appeared to have been absorbed after 1 h, suggesting relatively good absorption of both drugs. The liver-to-plasma ratio of entospletinib and lanraplenib was not meaningfully affected by the ABC transporters in any of the tested strains (Suppl. Fig. 3).

3.3. Drug-drug interaction with combined drug administration

The single administration arm in wild-type mice was taken along in case there was some form of drug-drug interaction between

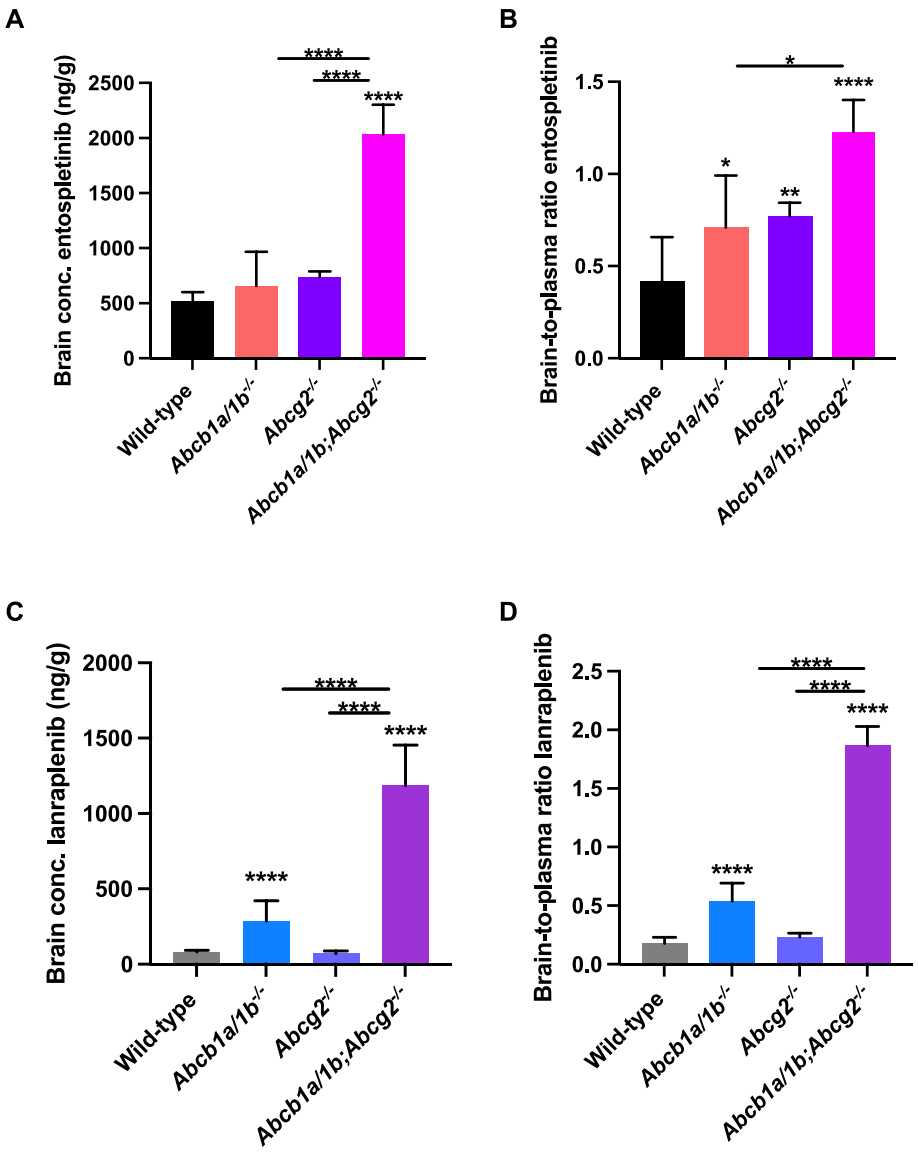

Fig. 2. Brain distribution of 10 mg/kg entospletinib and 10 mg/kg lanraplenib in female wild-type, *Abcb1a/b*$^{-/-}$, *Abcg2*$^{-/-}$ and *Abcb1a/b;Abcg2*$^{-/-}$ mice 1 h after oral administration of both drugs simultaneously ($n = 6$/group). **A.** Brain concentration entospletinib. **B.** Brain-to-plasma ratio entospletinib. **C.** Brain concentration lanraplenib. **D.** Brain-to-plasma ratio lanraplenib. Data are presented as mean ± SD. *, $P < 0.05$; **, $P < 0.01$; ****, $P < 0.0001$ compared to wild-type mice or as indicated by the bars.

entospletinib and lanraplenib, although we did not expect this given the modest oral dosages used. However, there was a modest level of mutual drug-drug interaction, with lanraplenib causing a 2.6-fold increase in the entospletinib plasma AUC, and entospletinib causing a 2.9-fold increase in lanraplenib plasma AUC ($P < 0.0001$ for each, Fig. 3, Suppl. Table 1). As we are primarily interested in the impact of ABC transporters on relative tissue distribution of the drugs, and as we can readily correct for modest differences in plasma exposure, the combination administration arms were still fully analyzed (see above and below). Similar to the combined administration, the overall plasma exposure of the lanraplenib alone administration was slightly lower compared to that of entospletinib (1.9-fold lower in wild-type mice, Fig. 3B and D, Suppl. Table 1). These data suggest that in mice there is not a big difference in oral availability between entospletinib and lanraplenib using the applied formulation.

Importantly, there was no significant difference in brain-to-plasma ratio of entospletinib between wild-type mice administered with solely entospletinib and in combination with lanraplenib (Suppl. Fig. 4A-B, Suppl. Table 1). This suggests that lanraplenib itself does not markedly influence entospletinib brain penetration. Just as for entospletinib, the brain-to-plasma ratio of lanraplenib was not significantly influenced by the addition of entospletinib to the administered formulation in wild-type mice (Suppl. Fig. 4C-D). The percentage of dose recovered from the SIC was also not significantly changed for either entospletinib or lanraplenib when comparing single and combined administrations, in spite of the differences in plasma concentration (Suppl. Fig. 5). This illustrates that the intestinal absorption of both drugs was not substantially affected by the coadministration. The liver-to-plasma ratio also did not show meaningful differences between the single and the combined administrations of both drugs (Suppl. Fig. 6).

In summary, the plasma exposures of entospletinib and lanraplenib are mutually increased by their coadministration. Theoretically several mechanisms might be involved in this drug-drug interaction, like inhibition or saturation of enzymes metabolizing the drugs, or inhibition or saturation of (uptake or efflux) transporters involved in limiting absorption or mediating elimination of the drugs. However, intestinal absorption was unlikely to be changed based on the SIC data (Suppl. Fig. 5). Abcb1 and Abcg2 appear to play only a minor role in the plasma

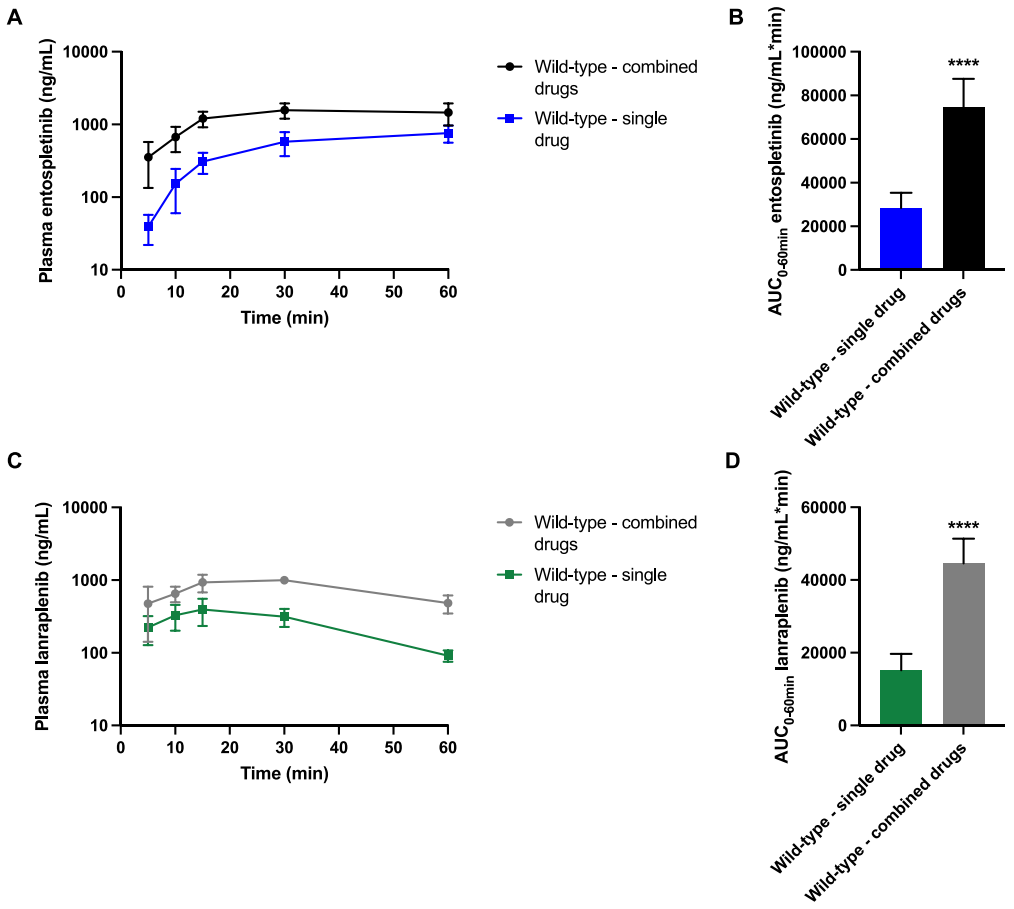

Fig. 3. Pharmacokinetic parameters of entospletinib and lanraplenib in female wild-type mice 1 h after oral administration of 10 mg/kg entospletinib and/or 10 mg/kg lanraplenib (single drug) or both drugs together (combined drugs). **A.** Plasma concentration-time curve of entospletinib (semi-log scale). **B.** $AUC_{0–60\ min}$ of entospletinib, area under the plasma concentration-time curve from 0 to the last time point ($t = 60$ min). **C.** Plasma concentration-time curve of lanraplenib (semi-log scale). **D.** $AUC_{0–60\ min}$ of lanraplenib. Data are presented as mean ± SD ($n = 6$/group). ****, $P < 0.0001$ compared to wild-type mice treated with the single drug solution.

exposure of both drugs based on the data in Fig. 1, so they are also unlikely to be involved in the observed drug-drug interaction (Fig. 3). The brain exposure of entospletinib and lanraplenib was markedly restricted by Abcb1a/b, whereas there is also a clear role for Abcg2 for both drugs. The intestinal and hepatobiliary excretion of entospletinib and lanraplenib are probably not substantially affected by the ABC transporters, although for lanraplenib there may be a small contribution to small intestinal content disposition.

3.4. Brain distribution of entospletinib and lanraplenib is boosted by the ABCB1/ABCG2 inhibitor elacridar

The brain penetration of both entospletinib and lanraplenib is restricted by Abcb1a/b and Abcg2. We therefore studied the possibility to enhance (boost) the tissue distribution of these drugs, especially for the brain, by the coadministration of the dual ABCB1/ABCG2 inhibitor elacridar in wild-type mice. The elacridar solution was administered 3 h prior to the (combined) entospletinib and lanraplenib solution to obtain maximal inhibition of the ABC transporters, based on the known T_{max} of elacridar of around 4 h after administration. As reference for the extent of in vivo inhibition of the ABC transporters, entospletinib and lanraplenib were also administered to *Abcb1a/1b;Abcg2*$^{-/-}$ mice.

The plasma pharmacokinetics ($AUC_{0–60min}$ and C_{max}) of entospletinib and lanraplenib were not significantly different between the three groups, in line with our earlier observation that Abcb1 and Abcg2 are not substantially involved in the plasma exposure of either drug (Suppl. Fig. 7, Suppl. Table 2). Coadministration of elacridar resulted in a strong enhancement of the brain concentration of entospletinib by 3.9-fold ($P < 0.0001$) and of lanraplenib by 14.6-fold ($P < 0.0001$) compared to the control wild-type group (Fig. 4A and C, Suppl. Table 2). The brain-to-plasma ratios were 3.7-fold ($P < 0.0001$) increased for entospletinib and 12-fold ($P < 0.0001$) for lanraplenib (Fig. 4B and D, Suppl. Table 2). The obtained brain exposure levels of entospletinib and lanraplenib in wild-type mice pretreated with elacridar were slightly lower than those in *Abcb1a/1b;Abcg2*$^{-/-}$ mice, albeit not statistically significant for entospletinib (Fig. 4, Suppl. Table 2). The brain-to-plasma ratio of lanraplenib in wild-type mice pretreated with elacridar was 36% lower ($P < 0.001$) compared to that in *Abcb1a/1b;Abcg2*$^{-/-}$ mice (Fig. 4D). Collectively, this suggests very extensive inhibition by elacridar of the ABC transporters at the BBB, although perhaps not fully complete with respect to transport of lanraplenib. In this elacridar boosting experiment, no signs of acute CNS toxicity were observed.

The liver disposition and the recovered percentage of dose in the small intestinal content of both entospletinib and lanraplenib were not meaningfully affected by the coadministration of elacridar (Suppl. Fig. 8 and 9). These findings are in line with our earlier observations that Abcb1a/1b and Abcg2 have little effect on the systemic pharmacokinetics of entospletinib and lanraplenib, while exerting a strong effect on their brain disposition.

3.5. OATP1a/1b does not influence liver or brain disposition of entospletinib and lanraplenib

In another 60 min experiment, we assessed the impact of the

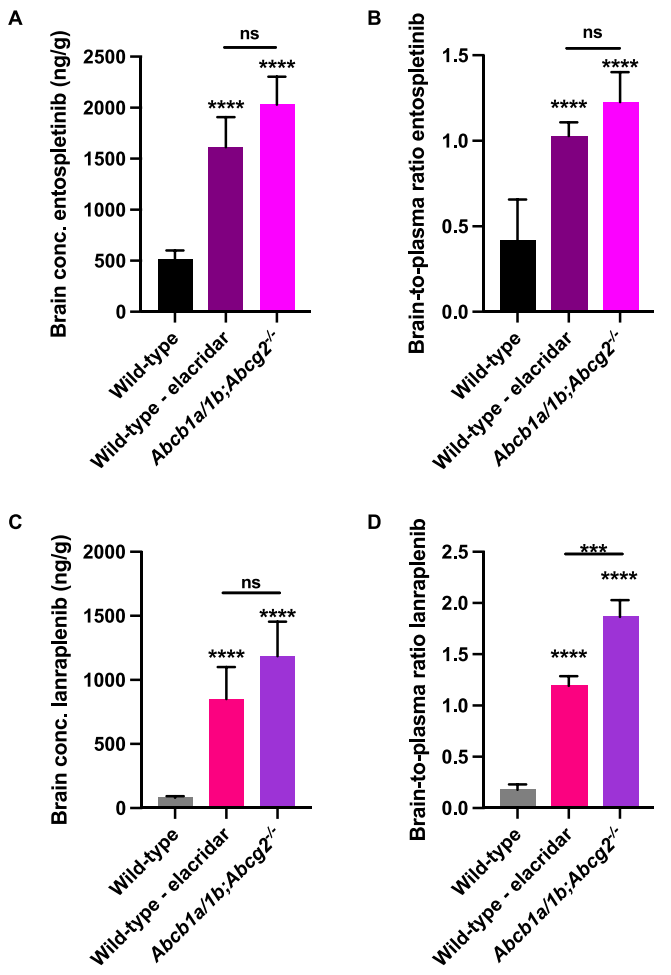

Fig. 4. Brain distribution of 10 mg/kg entospletinib and/or 10 mg/kg lanraplenib in female wild-type and *Abcb1a/b;Abcg2*$^{-/-}$ mice 1 h after oral administration of both drugs simultaneously and around 4 h after oral administration of 50 mg/kg elacridar (n = 6/group). **A.** Brain concentration entospletinib. **B.** Brain-to-plasma ratio entospletinib. **C.** Brain concentration lanraplenib. **D.** Brain-to-plasma ratio lanraplenib. Data are presented as mean ± SD. ns, not significant; ***, $P < 0.001$; ****, $P < 0.0001$ compared to wild-type mice or as indicated by the bar.

mOatp1a/1b uptake transporters on the pharmacokinetics of coadministered entospletinib and lanraplenib using female wild-type and *Oatp1a/1b*$^{-/-}$ mice. The plasma $AUC_{0–60min}$ and C_{max} of both drugs in *Oatp1a/1b*$^{-/-}$ mice were not significantly different from those in wild-type mice, suggesting there was no role for these uptake transporters in the plasma exposure of entospletinib and lanraplenib (Suppl. Fig. 10, Suppl. Table 3). Furthermore, the brain, liver, and SIC disposition of both entospletinib and lanraplenib were not substantially affected by the mOatp1a/1b transporters (Suppl. Fig. 11 and 12, Suppl. Table 3). Overall, there does not seem to be a noticeable role for mOatp1a/1b transporters in the plasma pharmacokinetics and tissue distribution of entospletinib and lanraplenib. It seems therefore unlikely that mOatp1a/1b transporters are involved in the observed drug-drug interaction between entospletinib and lanraplenib.

3.6. The plasma pharmacokinetics of lanraplenib are modestly restricted by mouse Cyp3a, but not human CYP3A4

The potential influence of Cyp3a and CYP3A4 on the net oral absorption and tissue disposition of entospletinib and lanraplenib (combined administration) was assessed in a 4-h study, using female wild-type, *Cyp3a*$^{-/-}$ and transgenic Cyp3aXAV mice (humanized mouse model; *Cyp3a*$^{-/-}$ mice with overexpression of human CYP3A4 in liver and small intestine). The plasma exposure of entospletinib was not significantly altered between the three mouse strains, indicating there is probably no role for CYP3A in the metabolism of entospletinib (Fig. 5A and B, Suppl. Table 4). Interestingly, the $AUC_{0\text{-}4h}$ of lanraplenib in *Cyp3a*$^{-/-}$ and Cyp3aXAV mice was significantly higher (both 2.0-fold, $P < 0.01$) compared to that in wild-type mice (Fig. 5C and D, Suppl. Table 4). A similar pattern was seen for lanraplenib plasma C_{max} (Suppl. Table 4). These data suggest modest involvement of mouse Cyp3a in the metabolic elimination of lanraplenib, but not of human CYP3A4. The analyzed tissues did not show meaningful differences between the strains when considering the tissue-to-plasma ratios (Suppl. Fig. 13 and 14). Collectively, these results suggest that the pharmacokinetics of entospletinib are not affected by Cyp3a/CYP3A4, but that the plasma exposure of lanraplenib is modestly restricted by one or more of the mouse Cyp3a enzymes, but not by human CYP3A4. Furthermore, given these results, the mutual drug-drug interaction between entospletinib and lanraplenib in combined administration is unlikely to be primarily related to the Cyp3a enzymes.

4. Discussion and conclusion

In this study, we demonstrated that upon oral administration of entospletinib and lanraplenib the short-term plasma exposure of both drugs is not significantly limited by Abcb1, whereas a minor indirect effect of Abcg2 cannot be excluded. The brain exposure of entospletinib and lanraplenib is restricted by both mouse Abcb1 and Abcg2, although for lanraplenib Abcb1 appears to dominate. Assuming that relative transport of entospletinib and lanraplenib would be similar for human ABCB1 and ABCG2, the relative impact of ABCG2 for both drugs in humans could be more prominent due to its higher abundance compared to ABCB1 in the human BBB vs that of mice (Bao et al., 2020; Liu, 2019). The relative brain distribution of both drugs does not seem to be influenced by their simultaneous administration. The restricted brain penetration of entospletinib could be completely reversed by coadministration of the dual ABCB1/ABCG2 inhibitor elacridar. Lanraplenib is a relatively more potent substrate for Abcb1 in the BBB compared to entospletinib, which may also be reflected in the not entirely complete reversal of its brain accumulation upon elacridar coadministration. Although elacridar is still not routinely applied in humans, it appears to be well tolerated based on clinical studies (Dash et al., 2017). Furthermore, the (direct) intestinal excretion and/or absorption of entospletinib was not significantly influenced by mAbcb1 and mAbcg2. For lanraplenib, there is possibly a minor role for Abcb1 in limiting the intestinal absorption.

This apparent discrepancy between the impact of ABC transporters on intestinal absorption and brain penetration of entospletinib and lanraplenib could be related to the higher drug exposure of intestinal Abcb1a and Abcg2 after oral drug administration compared to the exposure for BBB Abcb1a and Abcg2 from blood. Therefore, it is more likely that the intestinal ABC transporters will be (partly) saturated by the intestinal drug concentrations compared to the BBB ABC transporters. Moreover, the efficacy of the ABC efflux transporters in keeping drugs out of a certain compartment is to a large extent dependent on the effective influx rate of the drugs. The BBB is far more selective and allows only uptake of a very select group of nutrients, compared to the intestinal uptake of a large variety of nutrients using different uptake systems. Therefore, the intrinsic rate of intestinal drug uptake will generally be far higher than the uptake of drugs across the BBB, and thus more difficult to counteract by the ABC transporters.

The Oatp1a/b uptake transporters do not seem to affect the pharmacokinetics of entospletinib and lanraplenib and the CYP3A drug-metabolizing enzyme complex does not affect entospletinib pharmacokinetics. However, the plasma exposure of lanraplenib appears to be modestly restricted by mouse Cyp3a, but not human CYP3A4. A mutual drug-drug interaction between entospletinib and lanraplenib increases

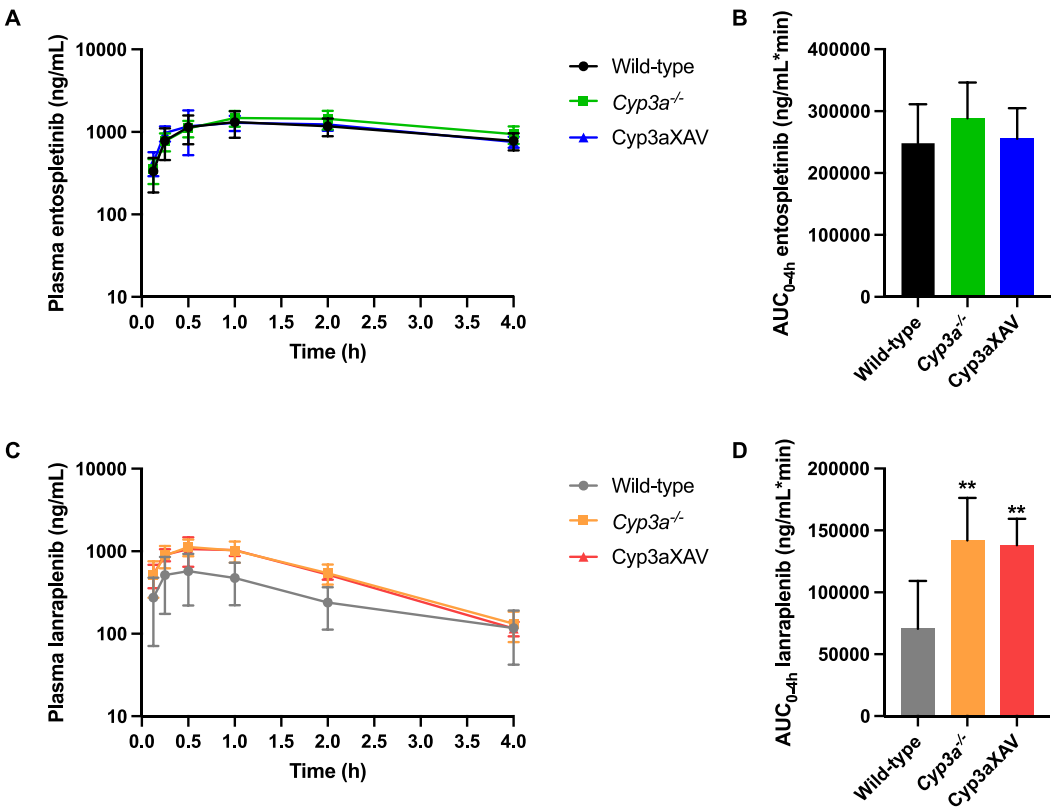

Fig. 5. Pharmacokinetic parameters in female wild-type, *Cyp3a*$^{-/-}$ and Cyp3aXAV mice 4 h after oral administration of 10 mg/kg entospletinib and 10 mg/kg lanraplenib simultaneously ($n = 6$/group). **A.** Plasma concentration-time curve of entospletinib (semi-log scale). **B.** $AUC_{0\text{-}4h}$ of entospletinib, area under the plasma concentration-time curve from 0 to the last time point ($t = 4$ h). **C.** Plasma concentration-time curve of lanraplenib (semi-log scale). **D.** $AUC_{0\text{-}4h}$ of lanraplenib. Data are presented as mean ± SD. **, $P < 0.01$ compared to wild-type mice.

their plasma exposure by 2.6- or 2.9-fold, but does not appear to be primarily mediated through ABCB1, ABCG2, OATP1a/1b, or CYP3A.

A previous in vitro study using lung cancer cells indicated that entospletinib is both a substrate and an inhibitor of human ABCG2. Usage of entospletinib could also result in downregulation of the ABCG2 protein. Therefore, entospletinib could theoretically be applied to overcome multidrug resistance in cancer treatment, when administered in combination with ABCG2 substrate anticancer drugs (Narayanan et al., 2021), such as mitoxantrone and doxorubicin. Furthermore, a PKPD study in healthy volunteers showed a 3- to 4-fold enhancement in entospletinib exposure after multiple dosing compared to single dosing. This might be due to a higher extent of entospletinib absorption caused by auto-inhibition (or saturation) of its intestinal metabolism or transport (Ramanathan et al., 2017). In the cited study, it was not further specified whether this auto-inhibition was related to ABCG2. However, based on the in vitro data, it could mean that entospletinib may alter the pharmacokinetics of other ABCG2 substrate drugs. This would also be in concordance with the previously observed entospletinib-dependent increase in rosuvastatin (an ABCG2 and OATP1B1/1B3 substrate) AUC in healthy volunteers. Therefore, coadministration of known ABCG2 substrates with entospletinib should be applied with caution. Our findings that entospletinib is in vivo transported by Abcg2 at the BBB would be compatible with the possibility that it can also inhibit Abcg2. In contrast, for lanraplenib it was previously unknown whether it is a transport substrate for ABCB1 and/or ABCG2 or not. Our data show that it is transported by both mouse Abcb1 and Abcg2 in vivo.

As a second question in this study, we aimed to investigate the possibility of simultaneously examining two drugs with related chemical structures and mechanism of action in our genetically modified mouse models. If feasible, this might reduce the number of mice needed in future experiments. However, our results show that there are significant complications with the simultaneous administration of the chosen two drugs at the selected dosages. Firstly, before the start of the experiment, we had expected that there would be minimal drug-drug interaction between entospletinib and lanraplenib, but our results showed the opposite. Their plasma exposures were both substantially enhanced by the combined administration. However, based on our results, it is unlikely that ABCB1, ABCG2, OATP1a/b and/or CYP3A are involved in the observed drug-drug interactions. Secondly, theoretically there may be an underestimation of the impact of Abcb1 and Abcg2 on the pharmacokinetics of entospletinib and lanraplenib when the drugs are simultaneously administered. If single administration had been applied in the different knockout strains, the influence of the ABC transporters might perhaps have been even more prominent than what we observed. Simply the nearly 3-fold higher plasma concentration of both drugs when combined, whatever the underlying cause, may have resulted in partial saturation of for instance ABC transporters, OATPs, or CYP3A metabolizing enzymes. This might then result in less pronounced differences than would otherwise have been seen.

Although the in vitro IC50 for SYK activity of entospletinib (~8 nM) is much lower than that of lanraplenib (~120 nM), highly divergent dosages have been reported for both drugs, with entospletinib dosed at 800 mg in humans (for treatment of B cell malignancies), versus lanraplenib at 30 mg (for lupus membranous nephropathy) (Currie et al., 2014; Blomgren et al., 2020; Ramanathan et al., 2017; Baker et al., 2020). This would translate to mouse equivalent dosages of ~130 mg/kg (entospletinib) vs ~5 mg/kg (lanraplenib) (Nair and Jacob, 2016). In theory, this might relate to a far better oral availability of lanraplenib. However, in mouse studies lanraplenib was administered in chow for treatment of lupus nephritis at an effective dosage of 250 mg/kg per day (Pohlmeyer et al., 2021). Given these very wide variations in dosages and species differences, we decided to give both drugs at the same

intermediate-low dosage, namely 10 mg/kg each. This approach prevents a gross asymmetry in possible drug-drug interactions and avoids solubility problems for the combined formulation. It also allows for a more balanced assessment of the in vivo interactions of both drugs with the various detoxifying proteins we aimed to study.

In summary, the brain penetration of entospletinib is restricted by both Abcb1 and Abcg2, while the brain distribution of lanraplenib is mainly restricted by Abcb1, with a less prominent role for Abcg2. Their impact in the BBB can be extensively reversed by coadministration of elacridar, which drastically enhances the brain disposition of both drugs in wild-type mice without any sign of acute toxicity. Based on these results, coadministration of strong ABCB1/ABCG2 inhibitors could enhance the brain exposure of entospletinib and lanraplenib. The results of this study may be beneficial for the further optimization of the safety and efficacy of entospletinib and lanraplenib during ongoing development and application. Furthermore, the idea of reducing the amount of mice needed in animal experiments by examination of two drugs at the same time could still be a possibility. However, this method needs further optimization and validation, and additional specific drug combinations need to be assessed. The therapeutic exposure of entospletinib in humans is relatively similar to what we observed in mice ($AUC_{0\text{-}48h}$ = 5834 ng·h/mL in human vs. $AUC_{0\text{-}4h}$ = 4139 ng·h/mL in mice) (Ramanathan et al., 2017). However, the mouse $AUC_{0\text{-}4h}$ of lanraplenib was much higher compared to the $AUC_{0\text{-}24h}$ in human (1178 vs. 13.96 ng·h/mL) (Blomgren et al., 2020). Therefore, retrospectively, lower dosages could have been considered to reduce the chance of drug-drug interactions in our combination studies.

Author contribution

Nancy H.C. Loos: Conceptualization; Formal analysis; Investigation; Methodology; Visualization; Writing – original draft.

Rolf W. Sparidans: Sample bioanalysis; Visualization; Writing – review & editing.

Paniz Heydari: Contribution in bioanalytical method development; Writing – review & editing.

Viët Bui: Contribution in performing mouse experiments; Writing – review & editing.

Maria C. Lebre: Contributed the reagents, materials, and mice; Writing – review & editing.

Jos H. Beijnen: Supervision; Writing – review content.

Alfred H. Schinkel: Conceptualization; Supervision; Formal analysis; Writing – review & editing.

Funding source

This research did not receive any specific grant from funding agencies in the public, commercial, or not-for-profit sectors. Part of this research was funded by core funding of the Netherlands Cancer Institute.

Declaration of Generative AI and AI-assisted technologies in the writing process

During the preparation of this work the author(s) did not use AI and AI-assisted technologies in the writing process.

CRediT authorship contribution statement

Nancy H.C. Loos: Writing – original draft, Visualization, Methodology, Investigation, Formal analysis, Conceptualization. **Rolf W. Sparidans:** Writing – review & editing, Visualization, Methodology. **Paniz Heydari:** Writing – review & editing, Methodology. **Viët Bui:** Writing – review & editing, Investigation. **Maria C. Lebre:** Writing – review & editing, Resources. **Jos H. Beijnen:** Writing – review & editing, Supervision. **Alfred H. Schinkel:** Writing – review & editing, Supervision, Formal analysis, Conceptualization.

Declaration of competing interest

The authors declare the following financial interests/personal relationships which may be considered as potential competing interests:

This research group of A.H. Schinkel receives revenue from commercial distribution of some of the mouse strains used in this study. The other authors have nothing to declare related to this study.

Data availability

Data will be made available on request.

Appendix A. Supplementary data

Supplementary data to this article can be found online at https://doi.org/10.1016/j.taap.2024.116911.

References

Allen, J.D., et al., 1999. The mouse Bcrp1/Mxr/Abcp gene: amplification and overexpression in cell lines selected for resistance to topotecan, mitoxantrone, or doxorubicin. Cancer Res. 59 (17), 4237–4241.

Andorsky, D.J., et al., 2019. An open-label phase 2 trial of entospletinib in indolent non-Hodgkin lymphoma and mantle cell lymphoma. Br. J. Haematol. 184 (2), 215–222.

Baker, M., et al., 2020. Phase II, randomised, double-blind, multicentre study evaluating the safety and efficacy of filgotinib and lanraplenib in patients with lupus membranous nephropathy. RMD Open 6 (3).

Bao, X., et al., 2020. Protein expression and functional relevance of efflux and uptake drug transporters at the blood-brain barrier of human brain and glioblastoma. Clin. Pharmacol. Ther. 107 (5), 1116–1127.

Blomgren, P., et al., 2020. Discovery of Lanraplenib (GS-9876): a once-daily spleen tyrosine kinase inhibitor for autoimmune diseases. ACS Med. Chem. Lett. 11 (4), 506–513.

Choudhuri, S., Klaassen, C.D., 2006. Structure, function, expression, genomic organization, and single nucleotide polymorphisms of human ABCB1 (MDR1), ABCC (MRP), and ABCG2 (BCRP) efflux transporters. Int. J. Toxicol. 25 (4), 231–259.

Colucci, F., et al., 2000. A new look at Syk in alpha beta and gamma delta T cell development using chimeric mice with a low competitive hematopoietic environment. J. Immunol. 164 (10), 5140–5145.

Couto, N., et al., 2020. Quantitative proteomics of clinically relevant drug-metabolizing enzymes and drug transporters and their Intercorrelations in the human small intestine. Drug Metab. Dispos. 48 (4), 245–254.

Currie, K.S., et al., 2014. Discovery of GS-9973, a selective and orally efficacious inhibitor of spleen tyrosine kinase. J. Med. Chem. 57 (9), 3856–3873.

Dash, R.P., Jayachandra Babu, R., Srinivas, N.R., 2017. Therapeutic potential and utility of Elacridar with respect to P-glycoprotein inhibition: an insight from the published in vitro, preclinical and clinical studies. Eur. J. Drug Metab. Pharmacokinet. 42 (6), 915–933.

Devault, A., Gros, P., 1990. Two members of the mouse mdr gene family confer multidrug resistance with overlapping but distinct drug specificities. Mol. Cell. Biol. 10 (4), 1652–1663.

Dolton, M., S, S., Cheng, F.C., Robeson, M., Worth, A., Tarnowski, T., Ramanathan, S., Silverman, J.A., 2016. Meeting abstract ASCO Entospletinib drug interaction profile and mass balance. https://doi.org/10.1200/JCO.2016.34.15_suppl.e14097. Available from:

Giacomini, K.M., et al., 2010. Membrane transporters in drug development. Nat. Rev. Drug Discov. 9 (3), 215–236.

Goncalves, J., et al., 2018. Relevance of breast Cancer resistance protein to brain distribution and central acting drugs: a pharmacokinetic perspective. Curr. Drug Metab. 19 (12), 1021–1041.

Kalliokoski, A., Niemi, M., 2009. Impact of OATP transporters on pharmacokinetics. Br. J. Pharmacol. 158 (3), 693–705.

Lamba, J.K., et al., 2002. Genetic contribution to variable human CYP3A-mediated metabolism. Adv. Drug Deliv. Rev. 54 (10), 1271–1294.

Liao, C., et al., 2013. Selective inhibition of spleen tyrosine kinase (SYK) with a novel orally bioavailable small molecule inhibitor, RO9021, impinges on various innate and adaptive immune responses: implications for SYK inhibitors in autoimmune disease therapy. Arthritis Res. Ther. 15 (5), R146.

Liu, X., 2019. ABC family transporters. Adv. Exp. Med. Biol. 1141, 13–100.

Lolodi, O., et al., 2017. Differential regulation of CYP3A4 and CYP3A5 and its implication in drug discovery. Curr. Drug Metab. 18 (12), 1095–1105.

Miller, D.S., 2014. ABC transporter regulation by signaling at the blood-brain barrier: relevance to pharmacology. Adv. Pharmacol. 71, 1–24.

Mócsai, A., et al., 2006. Integrin signaling in neutrophils and macrophages uses adaptors containing immunoreceptor tyrosine-based activation motifs. Nat. Immunol. 7 (12), 1326–1333.

Mócsai, A., Ruland, J., Tybulewicz, V.L., 2010. The SYK tyrosine kinase: a crucial player in diverse biological functions. Nat. Rev. Immunol. 10 (6), 387–402.

Nair, A.B., Jacob, S., 2016. A simple practice guide for dose conversion between animals and human. J Basic Clin Pharm 7 (2), 27–31.

Narayanan, S., et al., 2021. The spleen tyrosine kinase inhibitor, Entospletinib (GS-9973) restores Chemosensitivity in lung Cancer cells by modulating ABCG2-mediated multidrug resistance. Int. J. Biol. Sci. 17 (10), 2652–2665.
Oesch, F., 2009. Importance of knowledge on drug metabolism for the safe use of drugs in humans. Drug Metab. Rev. 41 (3), 298–300.
Poe, J.C., et al., 2018. SYK inhibitor entospletinib prevents ocular and skin GVHD in mice. JCI. Insight 3 (19).
Pohlmeyer, C.W., et al., 2021. Characterization of the mechanism of action of lanraplenib, a novel spleen tyrosine kinase inhibitor, in models of lupus nephritis. BMC Rheumatol 5 (1), 15.
Ramanathan, S., et al., 2017. Pharmacokinetics, pharmacodynamics, and safety of Entospletinib, a novel pSYK inhibitor, following single and multiple Oral dosing in healthy volunteers. Clin. Drug Investig. 37 (2), 195–205.
Schinkel, A.H., Jonker, J.W., 2003. Mammalian drug efflux transporters of the ATP binding cassette (ABC) family: an overview. Adv. Drug Deliv. Rev. 55 (1), 3–29.
Schinkel, A.H., et al., 1996. P-glycoprotein in the blood-brain barrier of mice influences the brain penetration and pharmacological activity of many drugs. J. Clin. Invest. 97 (11), 2517–2524.
Sharman, J., et al., 2015. An open-label phase 2 trial of entospletinib (GS-9973), a selective spleen tyrosine kinase inhibitor, in chronic lymphocytic leukemia. Blood 125 (15), 2336–2343.
Szakács, G., et al., 2008. The role of ABC transporters in drug absorption, distribution, metabolism, excretion and toxicity (ADME-Tox). Drug Discov. Today 13 (9–10), 379–393.
Tang, S., Yu, Q., Ding, C., 2022. Investigational spleen tyrosine kinase (SYK) inhibitors for the treatment of autoimmune diseases. Expert Opin. Investig. Drugs 31 (3), 291–303.
Zanger, U.M., Schwab, M., 2013. Cytochrome P450 enzymes in drug metabolism: regulation of gene expression, enzyme activities, and impact of genetic variation. Pharmacol. Ther. 138 (1), 103–141.